Sensors and Materials, Vol. 34, No. 2 (2022) 653–660
MYU Tokyo

S & M 2838

TSL and OSL Properties of Cu-doped CaF_2 Ceramics Prepared by Spark Plasma Sintering

Takumi Kato,* Daisuke Nakauchi, Noriaki Kawaguchi, and Takayuki Yanagida

Nara Institute of Science and Technology (NAIST),
8916-5, Takayama-cho, Ikoma-shi, Nara 630-0192, Japan

(Received October 7, 2021; accepted November 17, 2021)

Keywords: CaF_2, Cu, ceramic, TSL, dosimeter

The thermally and optically stimulated luminescence (TSL and OSL) properties of Cu-doped CaF_2 ceramics synthesized by spark plasma sintering (SPS), as well as their scintillation and photoluminescence (PL) properties, were investigated. The PL and scintillation spectra showed emission peaks at 390 and 490 nm, which were ascribed to Cu^+ ions and Cu clusters, respectively, judging from the PL decay time constants. After X-ray irradiation, TSL and OSL were observed upon heating at 182 °C and irradiating light of 620 nm, respectively. The dominant luminescence centers in the TSL and OSL processes were considered to be Cu clusters. The 0.1% Cu-doped CaF_2 sample had a linear TSL response in the dose range from 0.01 to 1000 mGy.

1. Introduction

Phosphors with thermally or optically stimulated luminescence (TSL or OSL) properties are used for personal monitoring applications and in imaging plates.[1–3] When such phosphors electromagnetically interact with ionizing radiation, many holes and electrons are generated. Some of them instantaneously recombine at luminescence centers with an emission of photons (scintillation), and some others temporarily accumulate at trapping centers. Accumulated holes or electrons can be re-excited from trapping centers by stimulation with heat or light. After the release, electrons and holes recombine at luminescence centers, emitting luminescence called TSL or OSL. From the viewpoint of practical applications, wide dose linearity, a high detection limit, and low fading are required for TSL and OSL properties. In particular, if the aim is to monitor a personal dose, it is desired that the effective atomic number (Z_{eff}) of the phosphor is similar to that of human soft tissue (Z_{eff} = 7.13) in terms of bioequivalence. Hence, for such dosimetry, the phosphor should be composed of light elements. Actually, commercially available personal dosimeters are equipped with phosphors with relatively low Z_{eff};[4] for instance, $Li_2B_4O_7$ and Al_2O_3 are used as TSL dosimeters.[5,6] Various investigations have been performed to improve the TSL or OSL characteristics by preparing several phosphors using different methods.

*Corresponding author: e-mail: kato.takumi.ki5@ms.naist.jp
https://doi.org/10.18494/SAM3682

ISSN 0914-4935

CaF_2 has been applied to optical lenses for high-power lasers, astronomical telescopes, and industrial inspection equipment due to its wide band gap and high durability. In the radiation measurement field, CaF_2 materials doped with Dy, Tm, or Mn are commercially available as TSL dosimeters, denoted TLD-200, 300, and 400, respectively, because of their low Z_{eff} and high sensitivity.[7–9] In addition to these TSL properties, it was also reported that CaF_2 materials doped with rare-earth or transition metal ions exhibit OSL properties, although they are not commercially available.[10,11]

In this study, CaF_2 ceramics doped with Cu were sintered in a spark plasma sintering (SPS) furnace, and then their TSL and OSL properties were studied to evaluate their potential use as dosimeters. In addition, their scintillation and photoluminescence (PL) properties were studied to reveal the origins of the luminescence centers. Although the TSL properties of Cu-doped CaF_2 single crystals were previously examined by Prokert and Sommer,[12] Pradhan,[13] and Sono and McKeever,[14] they concluded that the examined material included Ho as an unexpected impurity that determined the TSL properties of Cu-doped CaF_2, and that the material should more accurately be called Ho-doped CaF_2. In addition to these examinations, Zahedifar and Sadeghi reported the TSL properties of Cu-doped CaF_2 in the form of nanoparticles;[15] however, bulk materials are preferable to nanoparticles for practical use. Therefore, we investigated the TSL and OSL properties of Cu-doped CaF_2 ceramics as bulk materials in this study.

2. Materials and Methods

The ceramic samples were prepared in the same way as in our previous reports.[16,17] The wide surfaces of the obtained samples were mechanically polished with a polishing machine (MetaServ 250, BUEHLER) to standardize their thicknesses to about 1.50 mm.

To reveal the luminescence centers in the samples, scintillation spectra were measured by our original setup.[18] Moreover, PL excitation/emission spectra and decay curves were measured using a spectrofluorometer (FP8600, JASCO) and a Quantaurus-τ spectrometer (C11367-04, Hamamatsu), respectively.

To evaluate OSL dose response functions, we measured the OSL spectra and curves using the above spectrofluorometer. TSL glow curves were measured by a commercial TSL reader (TL-2000, Nanogray).[19] The heating rate was fixed to 1 °C/s for all the glow curve measurements. Furthermore, measurements of TSL spectra were performed using a CCD-based spectrometer (QE Pro, Ocean Optics) and a temperature controller/power supply (SCR-SHQ-A, SAKAGUCHI E.H VOC) at a constant temperature.[20] In the above measurements, an X-ray generator (XRB80N100/CB, Spellman) was used as a radiation source, which was equipped with an X-ray tube with a W anode target. We used an X-ray ionization chamber (TN30013, PTW) to determine the dose during the irradiation.

3. Results and Discussion

Figure 1 shows the X-ray-induced scintillation spectra of all the samples. In the 0.01% Cu-doped sample, a main emission peak was detected at 300 nm. In contrast, the 0.1 and 1.0% Cu-

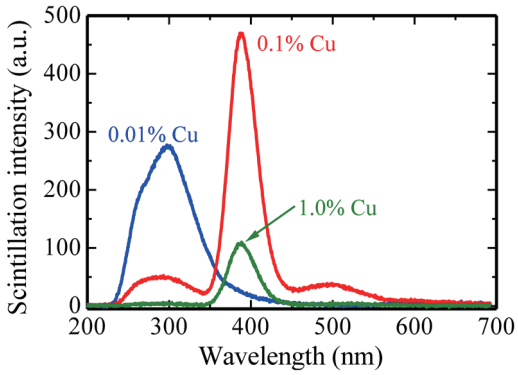

Fig. 1. (Color online) X-ray-induced scintillation spectra of all the samples.

doped samples showed emission peaks at 390 and 490 nm in addition to the emission peak at 300 nm. The origin of the emission peak at 300 nm is known to be self-trapped excitons (STEs), which are also observed in undoped CaF_2.[21] As the Cu concentration increased, the peak intensity at 300 nm decreased. According to a previous report, this result may be due to the local structure of the host lattice being affected by the increase in dopant concentration, thus suppressing the generation of STEs.[22] Moreover, the emission peaks at 390 and 490 nm were newly observed upon Cu doping, and the emission peak at 390 nm was dominant in the 0.1 and 1.0% Cu-doped samples.

Figure 2 shows PL excitation and emission spectra of the 0.1% Cu-doped sample when the monitored emission wavelengths were (a) 390 and (b) 490 nm. In the excitation spectrum monitored at 390 nm, excitation peaks were detected at 235 and 280 nm. On the other hand, an excitation peak was detected at 310 nm when the monitored emission wavelength was 490 nm. Figure 3 shows PL decay curves of the 0.1% Cu-doped sample excited at wavelengths of (a) 280 and (b) 315 nm. When the excitation wavelengths were 280 and 315 nm, the monitored emission wavelengths were 390 and 490 nm, respectively. The PL decay curve monitored at 390 nm was reproduced by an exponential decay function, and the derived decay time constant was 161 ns. In contrast, the PL decay curve monitored at 490 nm was approximated by a sum of two exponential decay functions, and the obtained decay time constants were 48 and 395 μs. Prior research revealed that typical Cu-doped phosphors have two decay time constants of microsecond order due to the $3d^9 4s^1$–$3d^{10}$ transition of Cu^+ ions.[23–26] In our measurements, such values were obtained for the PL decay curves monitored at 490 nm. Thus, we assigned the origin of the 490 nm peak to the $3d^9 4s^1$–$3d^{10}$ transition of Cu^+ ions. The emission peak at 390 nm was considered to be due to Cu clusters by a process of elimination. It is known that Cu-doped phosphors show luminescence ascribed to Cu clusters as well as Cu^+ ions.[27,28]

Figure 4 shows OSL stimulation and emission spectra of the 0.1% Cu-doped sample. The samples were irradiated with 1000 mGy of X-rays before the measurements. A stimulation peak was observed at 620 nm, and a dominant OSL emission peak appeared at 390 nm under the 620 nm stimulation. Although we performed the same measurements for the 0.01 and 1.0% Cu-doped samples, no emission peak was observed since the emission intensity was very low. By

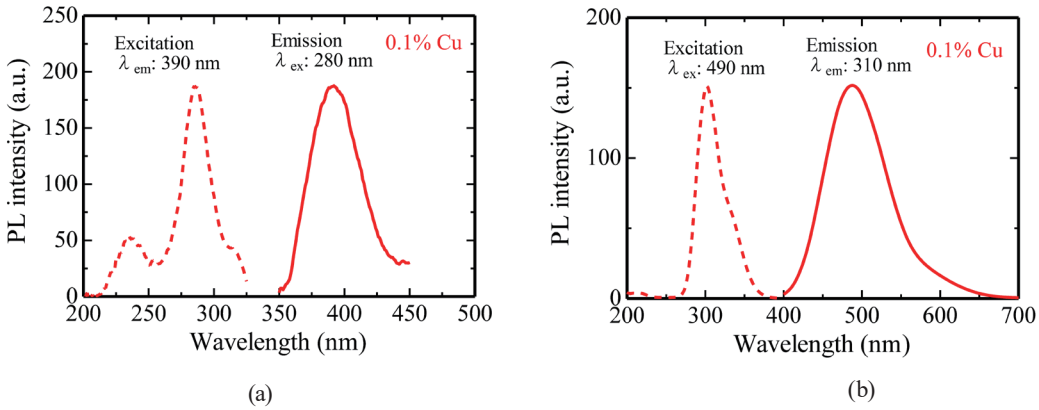

Fig. 2. (Color online) PL excitation and emission spectra of the 0.1% Cu-doped sample when the monitored emission wavelengths were (a) 390 and (b) 490 nm.

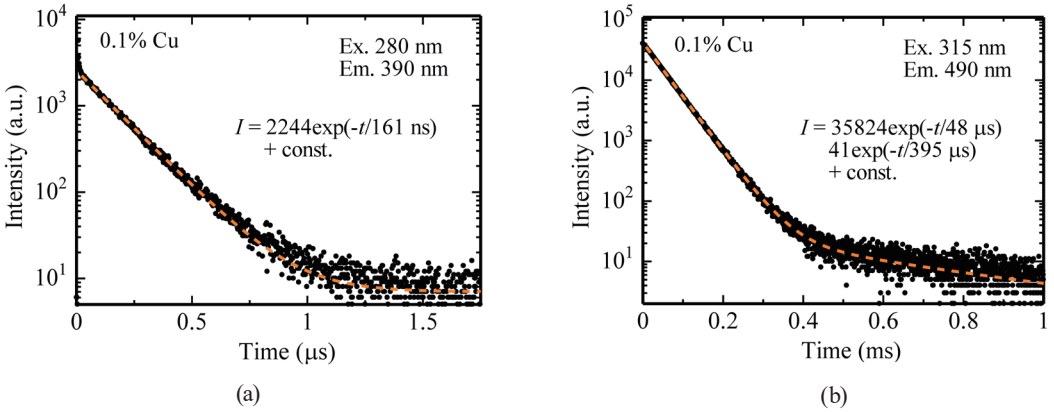

Fig. 3. (Color online) PL decay curves of the 0.1% Cu-doped sample excited at wavelengths of (a) 280 and (b) 315 nm.

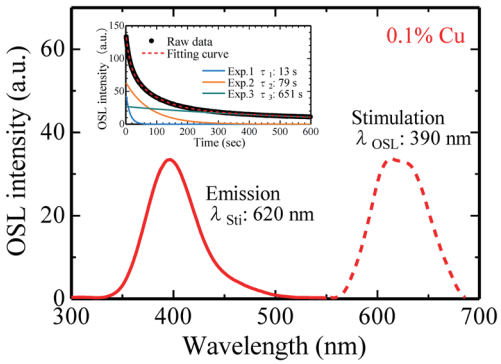

Fig. 4. (Color online) OSL stimulation and emission spectra of the 0.1% Cu-doped sample. The inset shows the OSL curve of the 0.1% Cu-doped sample measured during constant stimulation at 620 nm.

comparison with the results of scintillation and PL, the luminescence centers in the OSL process were concluded to be Cu clusters. Moreover, the trapping centers corresponding to the 620 nm stimulation are related to $(F_2^+)_A$ centers because of the absorption band observed at around 620 nm.[29] The inset in Fig. 4 shows the OSL curve of the 0.1% Cu-doped sample

measured during constant stimulation at 620 nm. The OSL curve was fitted by a sum of three exponential decay curves, and the obtained decay constants were 13, 79, and 651 s. Furthermore, the emission intensity decreased with the continuous stimulation. Therefore, the emission peak observed in Fig. 4 is clearly due to OSL. Note that this is the first report of Cu-doped CaF_2 exhibiting OSL. Figure 5 shows the OSL dose response function of the 0.1% Cu-doped sample. Here, the vertical axis represents the intensity of the OSL emission spectrum. The irradiation dose was varied from 0.01 to 1000 mGy, and the OSL signal was detected at doses of 10 mGy and above. The dynamic range of the Cu-doped sample if it were used as an OSL dosimeter was confirmed to be from 10 to 1000 mGy. The linearity was confirmed from the coefficient of determination (R^2) derived from a least-squares fitting of the experimental data with a power function ($y = ax^b$), and R^2 was 0.9993.

Figures 6(a) and 6(b) show TSL glow curves of all the samples and the TSL glow curve of the 0.1% Cu-doped sample with fitting analysis by a glow-curve decomposition (GCD) function,[30] respectively. The fitting parameters are summarized in Table 1. In this analysis, the free parameters are the maximum peak temperature (T_m), the maximum peak intensity (I_m), and the activation energy (E). Moreover, the frequency factor (S) was calculated from the above

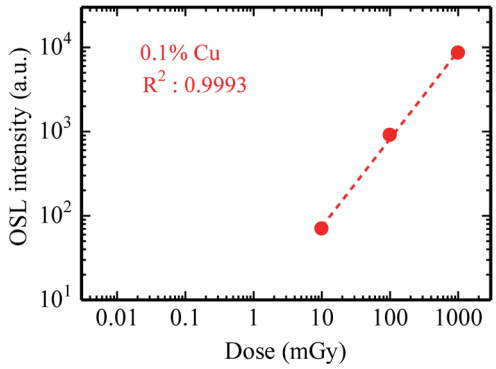

Fig. 5. (Color online) OSL dose response function of the 0.1% Cu-doped sample.

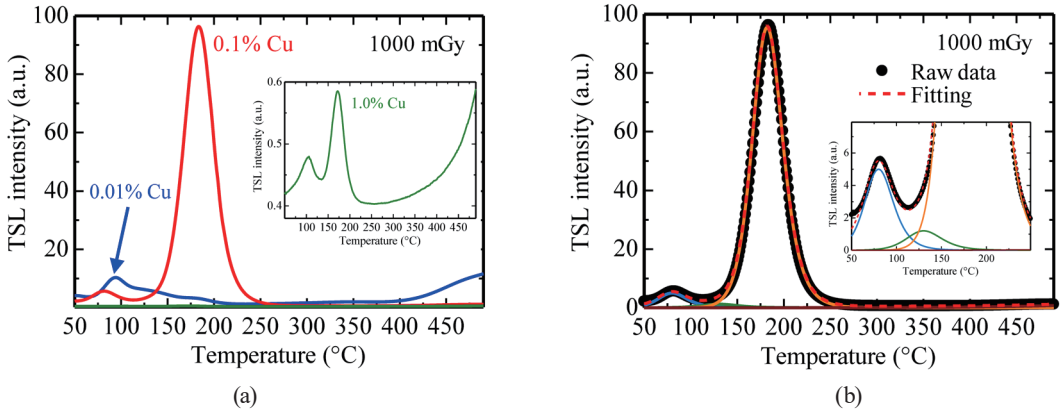

(a) (b)

Fig. 6. (Color online) (a) TSL glow curves of all the samples. (b) TSL glow curve of the 0.1% Cu-doped sample with fitting analysis by a GCD function.

Table 1
Fitting parameters for the TSL glow curve of the 0.1% Cu-doped sample.

	Peak 1	Peak 2	Peak 3
T_m (°C)	80	130	182
I_m (a.u.)	5.0	1.2	95.5
E (eV)	0.96	1.00	1.55
S (s^{-1})	1.51×10^{15}	8.63×10^{13}	5.55×10^{18}

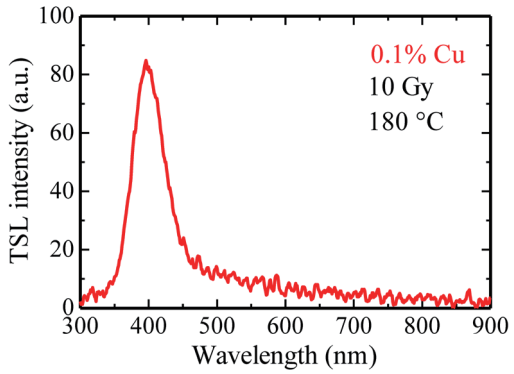

Fig. 7. (Color online) TSL spectrum of the 0.1% Cu-doped sample upon heating at the temperature of the highest TSL intensity in the glow curve.

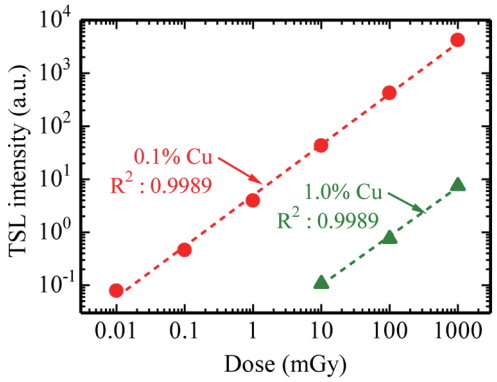

Fig. 8. (Color online) TSL dose response functions of the 0.1 and 1.0% Cu-doped samples. The TSL intensity was obtained by integrating the TSL signal of Peak 3.

parameters and the Boltzmann constant. The TSL glow curve of the 0.01% Cu-doped sample resembled that of undoped CaF_2 and was detected with a glow peak centered at 100 °C.[21] On the other hand, the glow curve of the 0.1% Cu-doped sample was best fitted by three GCD functions, and this sample showed glow peaks at 80, 130, and 182 °C. The prominent peak at 182 °C and a weak peak at 130 °C were also observed for Cu-doped CaF_2 nanoparticles, and this result was consistent with the previous report.[15] The trapping centers corresponding to 130 and 182 °C are currently under investigation and their discussion is beyond the scope of this paper.

Figure 7 shows the TSL spectrum when the 0.1% Cu-doped sample was heated at the temperature of the highest TSL intensity in the glow curve. As with the scintillation and OSL spectra, the 0.1% Cu-doped sample showed a main TSL peak at 390 nm. By the above argument, its origin is expected to be Cu clusters, and this result confirms that Cu clusters act as luminescence centers in the TSL process. Figure 8 depicts the TSL dose response functions of the 0.1 and 1.0 % Cu-doped samples. Here, the TSL intensity was obtained by integrating the TSL signal of Peak 3 in Fig. 6(b). The TSL responses of the 0.1 and 1.0% Cu-doped samples were confirmed to be linear with the X-ray irradiation dose from 0.01 to 1000 mGy and from 10 to 1000 mGy, respectively. The linearity was confirmed in the same manner as for the OSL, and the R^2 values of the 0.1 and 1.0% Cu-doped samples were both 0.9989. The TSL dose response function confirmed that the sensitivity of the 0.1% Cu-doped ceramic was higher than that of

Cu-doped CaF_2 nanoparticles.[15] Moreover, commercial TSL dosimeters such as Tb-doped Mg_2SiO_4 and Cu-doped $Li_2B_4O_7$ have a sensitivity of 0.01 mGy according to a previous study.[31] Therefore, the sensitivity of the present Cu-doped CaF_2 ceramic is equivalent to that of commercial TSL dosimeters.

4. Conclusions

Cu-doped CaF_2 ceramics were synthesized by SPS. Under X-ray irradiation, the ceramics showed scintillation peaks at 300, 390, and 490 nm. Their PL excitation/emission spectra and decay time constants indicated that the scintillation peaks at 390 and 490 nm were due to Cu^+ ions and Cu clusters, respectively. After X-ray irradiation, the Cu-doped CaF_2 ceramics also showed OSL caused by Cu clusters upon 620 nm stimulation. A similar emission peak was observed in the TSL spectrum. Furthermore, the Cu-doped CaF_2 ceramics showed TSL glow peaks at about 80, 130, and 182 °C, making it possible to measure radiation doses from 0.01 to 1000 mGy with an excellent linear response.

Acknowledgments

This work was supported by Grants-in-Aid for Scientific Research B (19H03533, 21H03733, and 21H03736) and Early-Career Scientists (20K15026 and 20K20104) from the Japan Society for the Promotion of Science. The Cooperative Research Project of the Research Center for Biomedical Engineering, Yashima Environment Technology Foundation, Okura Kazuchika Foundation, and Hitachi Metals-Materials Science Foundation are also acknowledged.

References

1 A. Boukhair, C. Heilmann, A. Nourreddine, A. Pape, and G. Portal: Radiat. Meas. **34** (2001) 513. https://doi.org/10.1016/S1350-4487(01)00218-9
2 D. Maruyama, S. Yanagisawa, Y. Koba, T. Andou, and K. Shinsho: Sens. Mater. **32** (2020) 1461. https://doi.org/10.18494/SAM.2020.2697
3 R. Oh, S. Yanagisawa, H. Tanaka, T. Takata, G. Wakabayashi, M. Tanaka, N. Sugioka, Y. Koba, and K. Shinsho: Sens. Mater. **33** (2021) 2129. https://doi.org/10.18494/sam.2021.3328
4 T. Kato, D. Shiratori, M. Iwao, H. Takase, D. Nakauchi, N. Kawaguchi, and T. Yanagida: Sens. Mater. **33** (2021) 2163. https://doi.org/10.18494/sam.2021.3318
5 N. Kawaguchi, G. Okada, Y. Futami, D. Nakauchi, T. Kato, and T. Yanagida: Sens. Mater. **32** (2020) 1419. https://doi.org/10.18494/SAM.2020.2752
6 S. Yanagisawa, D. Maruyama, R. Oh, Y. Koba, T. Andoh, and K. Shinsho: Sens. Mater. **32** (2020) 1479. https://doi.org/10.18494/SAM.2020.2698
7 A. Bos and J. Dielhof: Radiat. Prot. Dosimetry **37** (1991) 231. https://doi.org/10.1093/oxfordjournals.rpd.a081056
8 M. Danilkin, A. Lust, M. Kerikmäe, V. Seeman, H. Mändar, and M. Must: Radiat. Meas. **41** (2006) 677. https://doi.org/10.1016/j.radmeas.2006.04.020
9 A. Necmeddin Yazici, R. Chen, S. Solak, and Z. Yegingil: J. Phys. D. Appl. Phys. **35** (2002) 2526. https://doi.org/10.1088/0022-3727/35/20/311
10 A. K. Bakshi, B. Dhabekar, N. S. Rawat, S. G. Singh, V. J. Joshi, and V. Kumar: Nucl. Instrum. Methods Phys. Res., Sect. B **267** (2009) 548. https://doi.org/10.1016/j.nimb.2008.12.007
11 F. Nakamura, T. Kato, G. Okada, N. Kawaguchi, K. Fukuda, and T. Yanagida: Ceram. Int. **43** (2017) 604. https://doi.org/10.1016/j.ceramint.2016.09.201

12 K. Prokert and M. Sommer: Radiat. Prot. Dosimetry **78** (1998) 249. https://doi.org/10.1093/oxfordjournals.rpd.a032357
13 A. S. Pradhan: Radiat. Prot. Dosimetry **100** (2002) 289. https://doi.org/10.1093/oxfordjournals.rpd.a005870
14 D. A. Sono and S. W. S. McKeever: Radiat. Prot. Dosimetry **100** (2002) 309. https://doi.org/10.1093/oxfordjournals.rpd.a005875
15 M. Zahedifar and E. Sadeghi: Radiat. Prot. Dosimetry **157** (2013) 303. https://doi.org/10.1093/rpd/nct151
16 F. Nakamura, T. Kato, G. Okada, N. Kawaguchi, K. Fukuda, and T. Yanagida: J. Eur. Ceram. Soc. **37** (2017) 4919. https://doi.org/10.1016/j.jeurceramsoc.2017.06.010
17 T. Kato, D. Nakauchi, N. Kawaguchi, and T. Yanagida: Mater. Lett. **270** (2020) 127688. https://doi.org/10.1016/j.matlet.2020.127688
18 T. Yanagida, K. Kamada, Y. Fujimoto, H. Yagi, and T. Yanagitani: Opt. Mater. **35** (2013) 2480. https://doi.org/10.1016/j.optmat.2013.07.002
19 T. Yanagida, Y. Fujimoto, N. Kawaguchi, and S. Yanagida: J. Ceram. Soc. Jpn. **121** (2013) 988. https://doi.org/10.2109/jcersj2.121.988
20 G. Okada, T. Kato, D. Nakauchi, K. Fukuda, and T. Yanagida: Sens. Mater. **28** (2016) 897. https://doi.org/10.18494/SAM.2016.1357
21 F. Nakamura, T. Kato, G. Okada, N. Kawaguchi, and K. Fukuda: J. Eur. Ceram. Soc. **37** (2017) 1707. https://doi.org/10.1016/j.jeurceramsoc.2016.11.016
22 Y. Lan, B. Mei, W. Li, F. Xiong, and J. Song: J. Lumin. **208** (2019) 183. https://doi.org/10.1016/j.jlumin.2018.12.047
23 J. A. Jiménez: J. Phys. Chem. Solids **85** (2015) 212. https://doi.org/10.1016/j.jpcs.2015.05.022
24 G. D. Patra, M. Tyagi, D. G. Desai, B. Tiwari, S. Sen, and S. C. Gadkari: J. Lumin. **132** (2012) 1101. https://doi.org/10.1016/j.jlumin.2011.12.005
25 D. Shiratori, Y. Isokawa, N. Kawaguchi, and T. Yanagida: Sens. Mater. **31** (2019) 1281. https://doi.org/10.18494/SAM.2019.2188
26 H. Kimura, T. Kato, D. Nakauchi, N. Kawaguchi, and T. Yanagida: Sens. Mater. **33** (2021) 2187. https://doi.org/10.18494/sam.2021.3322
27 S. K. Sharma, S. S. Pitale, M. M. Malik, T. K. GunduRao, S. Chawla, M. S. Qureshi, and R. N. Dubey: J. Lumin. **130** (2010) 240. https://doi.org/10.1016/j.jlumin.2009.08.014
28 H. Ikeda, T. Murata, and S. Fujino: Mater. Chem. Phys. **162** (2015) 431. https://doi.org/10.1016/j.matchemphys.2015.06.010
29 J. M. G. Tijero and F. Jaque: Phys. Rev. B. **41** (1990) 3832. https://doi.org/10.1103/PhysRevB.41.3832
30 G. Kitis, J. M. Gomez-Ros, and J. W. N. Tuyn: J. Phys. D. Appl. Phys. **31** (1998) 2636. https://doi.org/10.1088/0022-3727/31/19/037
31 B. C. Bhatt: Radiat. Prot. Enviro. **34** (2011) 6. https://doi.org/10.13070/rs.en.1.720